Proceedings of the 3rd IFAC Workshop on Automatic
Control in Offshore Oil and Gas Production, Esbjerg,
Denmark, May 30 - June 1, 2018

Th_A_Regular_Talk.5

Modeling and control of an inline deoiling hydrocyclone*

Tamal Das * **Johannes Jäschke** *

* *Norwegian University of Science and Technology, 7491 Trondheim,
Norway (e-mail: tamal.das@ntnu.no, johannes.jaschke@ntnu.no).*

Abstract: In subsea oil and gas production and processing, automatic control of operation is of
significant importance. Typically, processing in subsea fields involves separation of hydrocarbons
from water and rejection of water in an environmentally friendly way. Separators such as deoiling
hydrocyclones help achieve these objectives. However, control strategy for hydrocyclones is not
yet well established in the literature due to a lack of control oriented models for hydrocyclone. In
this work we present a model for hydrocyclone based on mass balance equations. Subsequently,
we propose a PI controller for controlling the water quality.

Keywords: hydrocyclone, deoiler, modeling, control

1. INTRODUCTION

In oil and gas processing fields, to reduce the oil content in
the produced water a common separation system is used,
which caters to streams from various wells. The separation
system usually consists of bulk separators, such as first and
second stage separators and high purity separators, such
as hydrocyclone and compact flotation unit (Ruud et al.,
2015). The bulk separators perform a crude separation of
oil from the produced water. However, the water from
these separators is not suitable for discharge in the sea
because the oil content in this water is much higher
than that allowed for discharge in the sea. Permissible
emission limits on water discharge are in the range of
$20 - 30\ ppm$ oil in water (OSPAR, 2001). Hence, in order
to further reduce the oil content, the produced water
is processed in hydrocyclones. The inline hydrocyclones
(HC) employ cyclonic forces to achieve g-forces much
higher than gravity by virtue of a swirl element in the
flow direction close to the feed. Typically, hydrocyclones
bring down the oil content in water to a range of $100 - 200$
ppm, which is further reduced to a range of $20 - 30\ ppm$
using a compact flotation unit.

The emission limits on discharged water has reinforced the
need for automatic control of HC operation. Automatic
control of processes requires dynamic models. In the lit-
erature for HC modeling, first principles based models
have attracted less focus in comparison to data driven
approaches (Durdevic et al., 2015). However, it has been
reported that data driven models often fail to cover a wide
range of operating conditions (Durdevic et al., 2017). In
real operating fields, HCs can be subjected to a wide vari-
ety of feeds with different inlet water qualities, especially
in oil and gas fields in which a common separation system
handles a network of wells and tie-in wells.

In this work we focus on developing a control oriented first
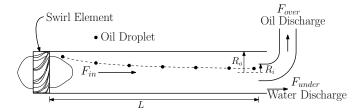principles based model for a deoiling inline hydrocyclone

Fig. 1. Schematic of an inline deoiling Hydrocyclone

in order to alleviate some of the challenges faced by data
driven models. An inline deoiling HC is shown in Figure
1, in which all the flows are co-current.

The inflow F_{in} containing oil and water enters the sepa-
rator and passes a swirl element. The separated water is
removed in the underflow F_{under}, and the oily concentrate
is taken out in the overflow F_{over}. We derive our dynamic
model based on mass balance for oil droplets. We extend
the previously developed steady state model by (Das et al.,
2016) to include dynamic behavior. In our model, the
separation of the oil droplets is governed by the radial and
axial velocities. We calculate the oil cut in F_{under} based
on a spatial profile of the oil droplets in the separator.
This spatial profile changes temporally under transient
conditions.

In this work, we use the dynamic model as plant to
propose a control loop from Oil in Water in processed
water flow F_{under} to oily discharge flow F_{over}. The rest
of the paper is organized in the following way: In section
2, we describe the process. Section 3 presents the model
equations. Section 4 describes the details of the controller
used to control water quality. Results are presented in the
section 5. The paper is concluded in the section 6.

2. PROCESS DESCRIPTION

In inline hydrocyclones, swirl elements are used to create
cyclonic effects. A typical swirl element is shown in Figure
2. The swirling effect is a function of the angle of the blades
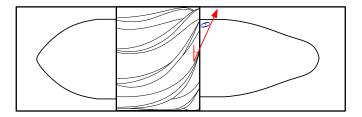
Fig. 2. Swirl element (Adapted from (Van Campen, 2014))

θ. This element is placed at the start of the hydrocyclone near feed as shown in Figure 1. This puts the flow in a swirl motion, which lets the fluids have an angular velocity as well as an axial velocity. Along the length of the separator towards the outlet the swirl decays. The density difference between oil and water propels dispersed oil droplets radially towards the center of the separator as the fluids move axially to the exit (shown in Figure 1).

3. HC MODELING

We model the HC assuming that the overflow F_{over}, the inlet total flow F_{in} and inlet oil cut ϵ_{in} are known. Because of the cyclonic forces and different axial flows in the two coaxial sections, the oil droplets have specific radial and axial velocities, which are functions of their size, their radial and axial positions inside the separator and the total flow rate. The droplets are assumed to immediately achieve terminal velocities in the radial direction. These velocities have a very spatially local validity, hence it is necessary to solve for the hydrodynamics in a spatial way.

It is assumed that based on the design given by radii R_i and R_o, the separator volume is segmented into two volumes, one inner cylindrical and one outer annular. The flows F_{over} and F_{under} flow in the inner and the outer volumes, respectively. Droplets, under the influence of the cyclonic forces, will travel radially inwards towards the center. The droplets crossing the common interface between these two volumes are going to switch from one outlet to the other. The cyclonic force is proportional to the square of the droplet size, hence the larger the droplets, the higher the possibility of them exiting in the oily discharge. The cyclonic effect produced by the swirl element is proportional to the F_{in}, however, this effect also causes droplets to break leading to several smaller droplets. Hence, the overall effect of increasing F_{in} on the achieved separation is given by a trade-off between the effects mentioned earlier.

For the model, some equations have been written as partial differential equations (PDE), which are discretized in radial and axial directions to obtain a series of ordinary differential equations. Other model equations have been written directly for the discretized control volumes as presented below.

3.1 Model equations (PDEs)

The coordinate system used for developing the model is shown in Figure 3. The r-coordinate starts at the center of the separator and ends at the separator wall i.e. $r = R_o$.
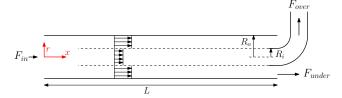

Fig. 3. Coordinate system and axial velocity profiles

The velocity of oil droplets in radial direction is denoted by v_r^d and in the axial direction is denoted by v_x^d. The axial velocity v_x^d is presented below as a function of r.

$$v_x^d(r) = \begin{cases} \dfrac{F_{over}}{\pi R_i^2} & \text{for } 0 \leq r \leq R_i \\ \dfrac{F_{under}}{\pi \left(R_o^2 - R_i^2\right)} & \text{for } R_i < r \leq R_o \end{cases} \quad (1)$$

The swirl number Ω is associated with the swirling effect the swirl element will produce. Ω is dependent on the θ in Figure 2. Values of Ω are between 2.5 and 7.5. We simulated our model for $\Omega = 2.5$, however other values could also be used. Here, we denote the maximum possible tangential velocity v_θ^{max} as a function of Ω and the bulk axial velocity $v_{x,b}$.

$$v_\theta^{max} = \Omega v_{x,b} \quad (2)$$

$$v_{x,b} = \frac{F_{in}}{\pi R_o^2} \quad (3)$$

The tangential velocities near $x = 0$ i.e. just downstream of the swirl element are dependent on the radial position as given below. The assumption of this velocity profile has been taken from (Tyvold, 2015). Here, R_c is the radius of the inner core with a solid body rotation. R_c/R_o is set to 0.25.

$$v_\theta^0(r) = \begin{cases} \dfrac{v_\theta^{max} r}{R_c} & \text{for } 0 \leq r \leq R_c \\ v_\theta^{max} & \text{for } R_c < r \leq R_o \end{cases} \quad (4)$$

However, we expect the swirling effect to decline in strength along the length of the separator. Hence, the tangential velocity v_θ shall decay exponentially with an exponent of C_{decay} along the length of the separator, thereby leading to the following steady state solution, as presented in (Najafi et al., 2011; Slot, 2013).

$$v_\theta(r, x) = v_\theta^0(r) \, exp\left(-\frac{C_{decay} x}{2 R_o}\right) \quad (5)$$

The above equation is empirical in nature. A possible unsteady extension of (5) is below, though this equation needs experimental validation.

$$\frac{\partial v_\theta}{\partial t} + v_x \frac{\partial v_\theta}{\partial x} = -\frac{C_{decay}}{2 R_o} v_\theta v_x \quad (6)$$

Here, (4) acts as the boundary condition for (6). The tangential velocity is going to give rise to a radial acceleration g_r, which is derived using centripetal acceleration. This radial acceleration can be used to derive the expression for local radial terminal velocity v_r the droplets will achieve. The expression comes from application of Stokes' law.

$$g_r(r, x) = \frac{(v_\theta(r, x))^2}{r} \quad (7)$$

$$v_r^d(r, x, d_d) = \frac{g_r(r, x) \, d_d{}^2 \, (\rho_w - \rho_o)}{18\mu_w} \quad (8)$$

Here, ρ_w, ρ_o and μ_w denote water density, oil density and water viscosity. The droplet diameter d_d is a function of the maximum possible tangential velocity v_θ^{max} as given below, which (Tyvold, 2015) provided using experimental data points found in (Van Campen, 2014).

$$d_d\left(v_\theta^{max}\right) \; [\mu m] = \begin{cases} \left(600 - 107 v_\theta^{max}\right) & \text{for } 0 \le v_\theta^{max} \le 4.45 \\ \left(160 - 8 v_\theta^{max}\right) & \text{for } 4.45 < v_\theta^{max} \le 20 \end{cases}$$
$$(9)$$

Since, v_θ^{max} is a function of the inflow F_{in}, F_{in} affects the droplet size and thereby also affects the v_r^d. Since, the model is spatial in nature, we do not expect the droplets throughout the separator to change size immediately when the flow changes. Hence, we consider a partial differential equation for the transit of droplet sizes through the separator.

$$\frac{\partial d_d}{\partial t} + v_x \frac{\partial d_d}{\partial x} = 0 \quad (10)$$

(10) shall result in the same evolution of average droplet diameter along the length of the separator as if solved for using population balances of different droplet classes, albeit with a much simpler equation. Here, (9) acts as boundary condition for (10) at $x = 0$.

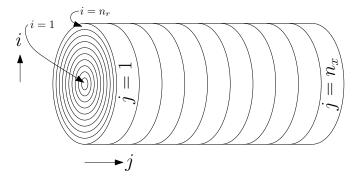*3.2 Discretization and equations for discretized volumes*

Fig. 4. Discretizations

In order to solve the model, we chose to discretize the separator volume in several control volumes. We consider $n_x = 12$ equally discretized volumes in the axial direction. Each of this axially dicretized volume is further discretized into $n_r = 12$ radial discretizations, with each control volume having the same volume. This resulted in a total of 144 control volumes as shown in Figure 4, where j denotes index in x direction and i denotes index in r direction starting from $r = 0$ and ending at $r = R_o$. Figure 5 shows one such ring element with the corresponding notation. Based on the control volume denoted by (i, j), the radial and axial boundaries of the control volumes are calculated as below.

$$r_{inner} = R_o \sqrt{\frac{i-1}{n_r}} \quad (11)$$

$$r_{outer} = R_o \sqrt{\frac{i}{n_r}} \quad (12)$$
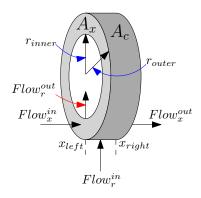
$$x_{left}(i) = (j-1) \frac{L}{n_x} \quad (13)$$

Fig. 5. Schematic of a single control volume

$$x_{right}(i) = \frac{L}{n_x} j \quad (14)$$

Equations (6) and (10) have been discretized using the finite volume method assuming d_d and v_θ are piecewise constant in each control volume. Further, it is assumed that the oil volume fractions are piecewise constant in each control volume. The droplets enter from the left boundary (x_{left}) and the radially outer boundary (r_{outer}) and leave from the right boundary (x_{right}) and the radially inner boundary (r_{inner}) as shown in Figure 5. The balance on oil volume for an arbitrary control volume (i, j) is written in the discretized form as below (We do not provide partial differential equations for these ones).

$$\overbrace{\frac{d}{dt}\left(\epsilon_d A_x \triangle x\right)}^{Accumulation} = \overbrace{\left(A_c v_r^d \epsilon_d\right)|_{r_{outer}}}^{Flow_r^{in}} - \overbrace{\left(A_c v_r^d \epsilon_d\right)|_{r_{inner}}}^{Flow_r^{out}}$$
$$+ \underbrace{\left(A_x v_x^d \epsilon_d\right)|_{x_{left}}}_{Flow_x^{in}} - \underbrace{\left(A_x v_x^d \epsilon_d\right)|_{x_{right}}}_{Flow_x^{out}} \quad (15)$$

Here, ϵ_d represents the local volume fraction of oil. A_x and A_c are shown in Figure 5, where A_x denotes the annular area of each control volume, given by $\pi R_o^2/n_r$ (All control volumes have same A_x as per discretization) and A_c the curved area given by $A_c(r) = 2\pi r \triangle x$, where $\triangle x = L/n_x$. Since the control volume doesn't change size, we can rearrange equation (15) to get the following equation.

$$\frac{d\epsilon_d}{dt} = \frac{\left(A_c v_r^d \epsilon_d\right)|_{r_{outer}} - \left(A_c v_r^d \epsilon_d\right)|_{r_{inner}}}{A_x \triangle x}$$
$$+ \frac{\left(v_x^d \epsilon_d\right)|_{x_{left}} - \left(v_x^d n \epsilon_d\right)|_{x_{right}}}{\triangle x} \quad (16)$$

The boundary conditions for the x coordinate are related to the inlet conditions and therefore, they have been embedded in the control volumes at the left edge near the inlet, i.e. $\{(i, j) : j = 1, i = 2, \dots, (n_r - 1)\}$ as follows:

$$\frac{d\epsilon_d(i, j)}{dt} = \frac{v_x^d(x_{left}) \epsilon_{in} - v_x^d(x_{right}) \epsilon_d(i, j)}{\triangle x}$$
$$\frac{(A_c v_r^d)|_{r_{outer}} \epsilon_d(i+1, j)}{A_x \triangle x} - \frac{(A_c v_r^d)|_{r_{inner}} \epsilon_d(i, j)}{A_x \triangle x} \quad (17)$$

ϵ_{in} is inlet produced water oil cut. For the control volume $(i, j) = (n_r, 1)$, there is no radial flow in, hence, the following equation holds.

$$\frac{d\epsilon_d(i,j)}{dt} = \frac{-(A_c v_r^d)|_{r_{inner}} \epsilon_d(i,j)}{A_x \triangle x}$$
$$+ \frac{v_x^d(x_{left})\epsilon_{in} - v_x^d(x_{right})\epsilon_d(i,j)}{\triangle x} \qquad (18)$$

For the control volume $(i,j) = (1,1)$, there is no radial flow out, hence, the following equation holds.

$$\frac{d\epsilon_d(i,j)}{dt} = \frac{(A_c v_r^d)|_{r_{outer}} \epsilon_d(i+1,j)}{A_x \triangle x}$$
$$+ \frac{v_x^d(x_{left})\epsilon_{in} - v_x^d(x_{right})\epsilon_d(i,j)}{\triangle x} \qquad (19)$$

For the control volumes $\{(i,j) : i = n_r, j = 2, \ldots, n_x\}$, there is also no radial flow in. Hence, the following equations hold.

$$\frac{d\epsilon_d(i,j)}{dt} = -\frac{(A_c v_r^d)|_{r_{inner}} \epsilon_d(i,j)}{A_x \triangle x}$$
$$+ \frac{v_x^d(x_{left})\epsilon_d(i,j-1)}{\triangle x} - \frac{v_x^d(x_{right})\epsilon_d(i,j)}{\triangle x} \qquad (20)$$

For the control volumes $\{(i,j) : i = 1, j = 2, \ldots, n_x\}$, there is also no radial flow out. Hence, the following equations hold.

$$\frac{d\epsilon_d(i,j)}{dt} = \frac{(A_c v_r^d)|_{r_{outer}} \epsilon_d(i+1,j)}{A_x \triangle x}$$
$$+ \frac{v_x^d(x_{left})\epsilon_d(i,j-1)}{\triangle x} - \frac{v_x^d(x_{right})\epsilon_d(i,j)}{\triangle x} \qquad (21)$$

The rest of the equations can be written for the control volumes $\{(i,j) : j = 2, \ldots, n_x, i = 2, \ldots, (n_r - 1)\}$ as follows:

$$\frac{d\epsilon_d(i,j)}{dt} = \frac{v_x^d(x_{left})\epsilon_d(i,j-1)}{\triangle x} - \frac{v_x^d(x_{right})\epsilon_d(i,j)}{\triangle x}$$
$$\frac{(A_c v_r^d)|_{r_{outer}} \epsilon_d(i+1,j)}{A_x \triangle x} - \frac{(A_c v_r^d)|_{r_{inner}} \epsilon_d(i,j)}{A_x \triangle x} \qquad (22)$$

Note that in the above equations for computing the radial velocities at the interface between two radial control volumes, a volumetric averaging was performed.

3.3 Re-entrainment equations

The model presented so far is governed by two velocities, the v_r^d and v_x^d, where v_r^d has dependency on v_x^d. If we raise F_{in}, v_x^d will increase and therefore, also v_r^d will increase. d_d goes down for higher F_{in}, which reduces the v_r^d. The overall effect of F_{in} on separation is, therefore, a trade-off between the two effects mentioned earlier. We reckon that the separation performance will be affected by the magnitude of F_{in} as well as the difference between F_{over} and F_{under}. In this model, F_{over} is much lower than F_{under}. We made an oversimplified assumption of two plug flows based on these two flows. Two flows next to each other with very different velocities will have a tendency to intermix due to radial pressure gradients. It is expected that part of the impure F_{over} flow will exit with the underflow, which will cause worsening of the achieved separation in F_{under}. Hence, we expect an re-entrainment flow q_{re-en} as a function of the difference between the axial velocities achieved in the two flows as shown below.

$$q_{re-en} = k_{re-en} \left(\frac{F_{under}}{\pi(R_o^2 - R_i^2)} - \frac{F_{over}}{\pi R_i^2} \right) \qquad (23)$$

k_{re-en} is a re-entrainment constant, which is chosen as $1 \cdot 10^{-6} \ m^2$. Intuitively, larger the difference between overflow plug velocity and underflow plug velocity, larger the possibility of re-entrainment of one flow in the other. The above equation captures that effect. We assume here that the overflow is usually controlled to a flow of F_{over} using a flow controller. Hence, it follows that the loss of flow in overflow due to re-entrainment will be compensated by an equal amount of flow q_{re-en} from underflow to overflow.

3.4 Calculation of water quality

The model produces the oil volume fraction in the all the control volumes. These fractions can be used to compute the water quality of the outgoing F_{under} and F_{over} streams. To produce an estimate of the oil content, we employ the following equations.

$$\epsilon_{under}^{ideal} = \frac{A_x \sum_{i=4}^{n_r} v_x^d(r)\epsilon_d(i,n_x)}{F_{under}} \qquad (24)$$

ϵ_{under}^{ideal} is an estimate of the water quality in the underflow if no re-entrainment was happening. This variable is computed by summing up all the oil outflows that will exit in the radial section ($R_i < r \leq R_o$) for the control volumes on the rightmost edge ($j = n_x$) and dividing it by the underflow F_{under}. Since the radially outer edge of the control volume $(3, n_x)$ is at $r = R_i$, we account for underflow from the control volume $(4, n_x)$ to (n_r, n_x) and for overflow from $(1, n_x)$ to control volume $(3, n_x)$. Hence, we obtain the following expression for the ϵ_{over}^{ideal}.

$$\epsilon_{over}^{ideal} = \frac{A_x \sum_{i=1}^{3} v_x^d(r)\epsilon_d(i,n_x)}{F_{over}} \qquad (25)$$

To compute the real water quality of the underflow, which will be affected by the re-entrainment of the oil rich overflow into the underflow near the exit, we employ the following equation.

$$\epsilon_{under}^{real} = \frac{(F_{under} - q_{re-en})\epsilon_{under}^{ideal} + (q_{re-en})\epsilon_{over}^{ideal}}{F_{under}} \qquad (26)$$

The hydrocyclone model is developed assuming that $F_{over}/F_{in} > \epsilon_{in}$, which is most often the case. If, however, $F_{over}/F_{in} < \epsilon_{in}$, model could produce $\epsilon_{over}^{ideal} > 1$, which is physically not possible. This happens because the model has not been corrected for these special unrealistic scenarios. The correction would mean that the flows out of a donor control volume to a receiver control volume is dependent on the oil hold up of the receiver control volume. If the receiver control volume has an oil hold up close to 1, oil flows into the control volume will approach zero. This modification makes the model severely nonlinear. Hence, for simplicity we do not consider this effect.

3.5 Model parameters

The model parameters are presented in the table below:

Table 1. Model parameters

Parameter	Value	Unit
Outer radius, R_o	0.05	m
Inner radius, R_i	0.025	m
Inner core radius, R_c	0.0125	m
Separator length, L	1.7	m
Nominal inlet oil cut, ϵ_{in}	1500	ppm
Nominal inlet flow, F_{in}	100/3600	m^3/s
Nominal overflow, F_{over}	0.7/3600	m^3/s
Swirl number, Ω	2.5	-
Swirl decay coefficient, C_{decay}	0.04	-
Oil density, ρ_o	881	kg/m^3
Water density, ρ_w	1064	kg/m^3
Viscosity of brine, μ	10^{-3}	$Pa \cdot s$
Re-entrainment constant, k_{re-en}	$1 \cdot 10^{-6}$	m^2
Number of axial discretizations, n_x	12	-
Number of radial discretizations, n_r	12	-

4. CONTROL STRUCTURE

The model described previously has been considered as a plant for conducting dynamic simulations. Further, we used the model to test a simple PI control law for controlling the processed water oil cut given by ϵ_{under}^{real}. The control structure is shown in Figure 6, in which we consider inlet flow F_{in} and incoming oil cut ϵ_{in} as disturbances.
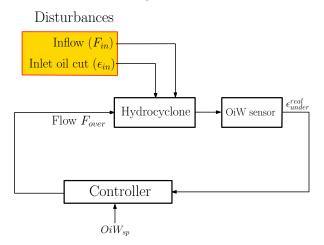

Fig. 6. HC control using OiW controller

The PI controller ($C(s)$) used for computing F_{over} from ϵ_{under}^{real} measurement and its set point OiW_{sp} is the following. The controller tunings have been derived using SIMC rules (Skogestad, 2003). Note that the controller takes values for ϵ_{under}^{real} in ppm.

$$C(s) = -4.8 \cdot 10^{-6} \left(1 + \frac{0.25}{s}\right) \quad (27)$$

5. RESULTS

The simulations were performed in MATLAB/Simulink. For finding the steady state, we used the fsolve solver in MATLAB, whereas for the dynamic simulations we used Simulink. The dynamic model was solved using the ode15s solver. The results will be presented in three segments. Firstly, we will present the steady state solution of the oil volume fractions over axial and radial positions for the nominal case using parameter values presented

in subsection 3.5. In the next segment we will present the dynamic open loop results showing the effect of the disturbances, F_{in} and ϵ_{in} and the manipulated variable F_{over} on the oil cut ϵ_{under}^{real} in underflow. In the last segment, we will present the dynamic closed loop results.

5.1 Steady state result

The steady state oil volume fractions are shown below.

Table 2. Steady state oil fractions

Oil frac. [$\times 10^{-2}$]	$j=1$	$j=4$	$j=8$	$j=12$
$i=1$	12.1366	38.0792	53.7138	59.3166
$i=3$	0.1475	0.1171	0.0666	0.0374
$i=4$	0.1475	0.1169	0.0663	0.0372
$i=8$	0.1345	0.0619	0.0174	0.0059
$i=12$	0.0548	0.0040	0.0003	0.0000

This clearly shows that the oil droplets are gradually moving towards the center ($i=1$) as they proceed towards the exit ($j=12$). Next, we present the oil flows out of different control volumes. This result is presented in terms of absolute volumetric flow rate of oil since the densities are considered to be constant.
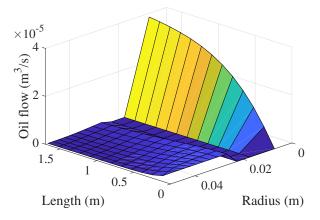

Fig. 7. Steady state spatial profile of oil flow

We see the radially inwards movement of oil in Figure 7 as it travels along the length of the separator. At each point in the length, the oil flows out of all radial discretizations add up to 0.4167×10^{-4} m^3/s. For the obtained steady state, the $\epsilon_{under}^{ideal} = 114.1$ ppm, $\epsilon_{under}^{real} = 147.0$ ppm and $\epsilon_{over}^{ideal} = 0.1981$.

5.2 Open-loop results

Open-loop results are presented in order to identify the response of changing disturbances, viz. F_{in} and ϵ_{in} on the underflow water quality ϵ_{under}^{real} in manual mode. We further present also the effect of changing the manipulated variable, the overflow F_{over} on the water quality. The open loop results can be seen in the Figure 8. When changing the F_{in}, three effects are in play, namely, reduction in residence time of the water inside the separator, increase in the tangential velocity and reduction in the droplet size. Of these effects, the droplet size reduction has the strongest effect. Reduced droplet size causes a reduction in radial velocity for the oil droplets. Hence, fewer droplets reach the overflow. Therefore, we see in Figure 8 that the
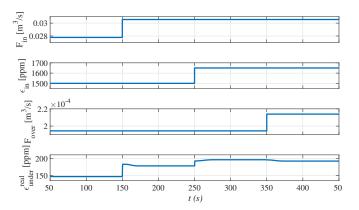
Fig. 8. Open loop behavior of the hydrocyclone model

oil content in the underflow rises. An increase in inlet oil content ϵ_{in} results in an increased oil content in the underflow, which is as expected. An increase in overflow F_{over} reduces the the oil content of the produced water. Hence, overflow is considered as a suitable manipulated variable for control design for controlling the water quality.
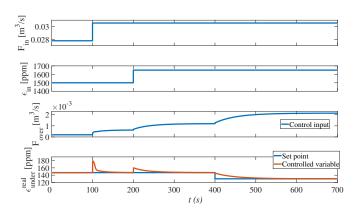
5.3 Closed-loop results

Fig. 9. Closed loop behavior of the hydrocyclone model

Based on the previous analysis, we chose F_{over} as our control input to control the underflow water quality ϵ_{under}^{real}. Here, we subject the system to disturbances, such as changes in inlet oil content and inflow and we try to maintain the controlled variable to a set point of 147 *ppm*. For the closed loop performance, see Figure 9. The controller acts quite rapidly when the inflow is raised by 10 %. It takes around 50 seconds before the controlled variable is brought back to the set point. A similar behavior is noticed when inlet oil content is raised by 10 %, in which water quality is off-spec for just around 50 seconds. Finally, we test the closed loop performance subject to a change in the set point from 147 to 130 *ppm*. The response time has been noted to be in the range of 100 seconds.

6. CONCLUSION

In this work, we developed a simplified dynamic model for an inline deoiling hydrocyclone. The model has been derived as a distributed parameter system to dynamically capture the oil content in the processed water. The model is able to study the impact of the disturbances and the

control input. However, note that (6) is empirical and needs further investigation to ensure validity. Further, a control scheme has been prescribed for controlling the processed water quality using the overflow. The controller tunings have been derived using the SIMC rules. The open loop behavior of the model is according to expectation. The performance of the control structure is satisfactory with response time for disturbance rejection in the range of 50 seconds, while that for a change in set point in the range of 100 seconds.

The modeling work has been conducted as an approach to control the processed water oil quality. A similar approach of modeling can be used to develop dynamic models for many other separators in which the separation is physically driven such as by gravity or cyclonic forces. For this model, we assume that the oil content can be measured online. The control structure that we designed will heavily depend on the reliability, accuracy and the response time of the Oil in Water sensors. For that, the results shown in (Durdevic et al., 2016) on the evaluation of Oil in Water sensors for control seem promising.

REFERENCES

Das, T., Tyvold, P.F., and Jäschke, J. (2016). Modelling and optimization of compact subsea liquid-liquid separation system. In *Computer Aided Chemical Engineering*, volume 38, 1255–1260. Elsevier.

Durdevic, P., Pedersen, S., and Yang, Z. (2016). Evaluation of oiw measurement technologies for deoiling hydrocyclone efficiency estimation and control. In *OCEANS 2016-Shanghai*, 1–7. IEEE.

Durdevic, P., Pedersen, S., Bram, M., Hansen, D., Hassan, A., and Yang, Z. (2015). Control oriented modeling of a de-oiling hydrocyclone. *IFAC-PapersOnLine*, 48(28), 291–296.

Durdevic, P., Pedersen, S., and Yang, Z. (2017). Challenges in modelling and control of offshore de-oiling hydrocyclone systems. In *Journal of Physics: Conference Series*, volume 783, 012048. IOP Publishing.

Najafi, A., Mousavian, S., and Amini, K. (2011). Numerical investigations on swirl intensity decay rate for turbulent swirling flow in a fixed pipe. *International Journal of Mechanical Sciences*, 53(10), 801–811.

OSPAR (2001). Discharges, ospar convention. URL www.ospar.org/work-areas/oic/discharges.

Ruud, T., Idrac, A., McKenzie, L., Høy, S., et al. (2015). All subsea: A vision for the future of subsea processing. In *Offshore Technology Conference*. Offshore Technology Conference.

Skogestad, S. (2003). Simple analytic rules for model reduction and pid controller tuning. *Journal of process control*, 13(4), 291–309.

Slot, J.J. (2013). *Development of a centrifugal in-line separator for oil-water flows*. University of Twente.

Tyvold, P.F. (2015). *Modeling and optimization of a subsea oil-water separation system*. Master's thesis, NTNU.

Van Campen, L.J.A.M. (2014). Bulk dynamics of droplets in liquid-liquid axial cyclones.